JOURNAL OF MATERIALS SCIENCE 17 (1982) 1595–1609

Electrical transport in light rare-earth orthochromites

A. K. TRIPATHI, H. B. LAL
Department of Physics, University of Gorakhpur, Gorakhpur 273001, India

Electrical conductivity, σ, Seebeck coefficient, S, and dielectric constant, ϵ, measurements on the pressed pellets of six light rare-earth orthochromites, $R CrO_3$, where R = La, Pr, Nd, Sm, Eu and Gd, have been carried out in the temperature range 300 to 1000 K. These are essentially electronic conductors, exhibiting p-type extrinsic semiconducting nature in the studied temperature range. The extrinsic charge carriers (holes) originate from Cr^{4+} centres which are present due to native defects in these solids. Their room-temperature electrical conductivities lie in the range 10^{-7} to 10^{-5} Ω^{-1} cm^{-1}, which become of the order of 10^{-2} Ω^{-1} cm^{-1} near 1000 K. The conductivity is a maximum in $LaCrO_3$ and drops across the $R CrO_3$ series, with $SmCrO_3$ being an exception. The mechanism involved in the electrical transport is the hopping of holes from Cr^{4+} centres to neighbouring Cr^{3+} ions. The activation energy of transport is nearly 0.3 eV. Typical hopping mobility of the holes is of the order of 10^2 cm^{-2} V^{-1} sec^{-1} at 325 K and of the order of 10 cm^2 V^{-1} sec^{-1} at 1000 K. The mobility activation energy of the holes in a typcial $R CrO_3$ decreases with temperature due to the smoothing of the potential barriers between Cr^{4+} and Cr^{3+} sites. Several discontinuities are observed in the σT against T^{-1} and S against T^{-1} plots of $R CrO_3$. The anomalies which these discontinuities reflect here have also been indicated.

1. Introduction

Rare-earth orthochromites, $R CrO_3$, where R is a rare-earth element, are typical perovskite-type compounds and crystallize in orthorhombically-distorted perovskite structures (space group $Pbnm$), having four formula units per unit cell [1–4]. This structure can also be looked upon as pseudocubic [3, 4]. The oxygen polyhedra surrounding the chromium ion in $R CrO_3$ is distorted and is believed to be the origin of the ferroelectricity inferred from pyroelectric current measurements in heavy members of the series [5]. Apart from the other physical properties, electrical transport studies on $R CrO_3$ are limited and conductivity data are available only for a few members of the series [6–13]. These have been found to have high electrical conductivities ($\sim$ 10^{-1} Ω^{-1} cm^{-1} at 1000 K) and their melting points are as high as approximately 2500 K [14]. Consequently, these are thought to be excellent electrode materials to be used in magneto hydrodynamic (MHD) power generating devices [9]. To exploit them in such devices it is essential to determine the basic electrical transport mechanism of pure $R CrO_3$.

This paper reports the electric transport behaviour of some light $R CrO_3$ (R = La, Pr, Nd, Sm, Eu and Gd) inferred from electrical conductivity, Seebeck coefficient, magnetoresistance and dielectric studies in the temperature range 300 to 1000 K. The study of $R CrO_3$ forms a part of a wider study of the electrical transport and magnetic properties of transition and rare-earth metal compounds covering rare-earth oxides [15, 16], molybdates [17–19], tungstates [20–23] and garnets [24, 25].

2. Material preparation and experimental procedure

The prepared samples were polycrystalline materials obtained from the high-temperature solid-state reaction between rare-earth sesquioxides R_2O_3 (of

0022–2461/82/061595–15$04.30/0

99.99% purity, from Fluka A.G., Switzerland) and Cr_2O_3 (of 99.99% purity, from Bonds, India). The orthochromities of La, Nd, Sm, Eu and Gd were obtained by mixing fine powders of the corresponding R_2O_3 and Cr_2O_3 in the correct molecular weight proportions, heated in air for nearly 24 h at a temperature of about 1500 K and then cooling slowly. The reaction taking place is

$$R_2O_3 + Cr_2O_3 \rightarrow 2\,RCrO_3. \quad (1)$$

However, in preparing $PrCrO_3$, the oxide Pr_6O_{11} (of 99.99% purity) was used. Undergoing the same process it forms $PrCrO_3$ at about 1650 K by the reaction

$$Pr_6O_{11} + 3\,Cr_2O_3 \rightarrow 6\,PrCrO_3 + O_2. \quad (2)$$

The prepared samples were checked by X-ray analysis using CuKα radiation ($\lambda = 0.15405$ nm): They were found to be single-phase and no part of the parent materials was found unreacted.

The prepared compounds were pressed, at a pressure greater than 6×10^8 N m^{-2} into pellets of circular cross-sectional area, $a \sim 0.90$ cm^2 and thickness, $t \sim 0.20$ cm (used in the conductivity, magnetoresistance and dielectric measurements) and $t \sim 0.70$ cm (used in the Seebeck coefficient measurements). The sample pellets were then sintered in air for about 24 h at about 1000 K. Sample holders used for σ and S measurements are described elsewhere [13, 26]. Samples were mounted between the rigid electrodes of the sample holder after coating with silver. The electrical conductivity, σ, measurement was carried out at applied a.c. signal frequencies of 10^2, 10^3 and 10^4 Hz using a Systronics LCR bridge (Type 921) in the temperature range 300 to 1000 K. The experimental values of σ were obtained within 2% accuracy. The Seebeck coefficient, S, measurement was also done in the same temperature range. However, the experimental values of S were obtained in general, to within ± 5% error. After the establishment of a constant thermal environment a temperature difference, ΔT, of ~ 10 or ~ 15° C was applied and correspondingly developed thermal e.m.f., ΔE across the sample was measured with a Keithley digital multimeter (type 171: internal impedance, $10^{10}\,\Omega$). The Seebeck coefficient, S, is the ratio of ΔE and ΔT. The measurement of dielectric constant, ϵ, was also carried out in the same temperature range employing the displacement method at an a.c. signal frequency of 10^3 Hz using the Systronics LCR bridge.

The magnetoresistance measurement was carried out at almost 450 K both in the transverse and longitudinal modes at variable uniform magnetic fields (0 to 1.28×10^6 A m^{-1}) obtained from an electromagnet Polytronic, Type EM 100. The sample holder used was the same but with smaller dimensions than the sample holder used in the conductivity measurement. In order to avoid difficulty in simultaneous regulation of the various components of the experimental set-up a direct measure of resistance of the sample, using the Keithley multimeter, was preferred.

3. Result

The studies have been performed on pressed circular pellets because it is difficult to prepare single-crystal and melt-solid polycrystalline materials due to their high melting points. In the pelletized material it is highly desirable to reduce the grain boundaries of increased resistance as much as be possible and to obtain a uniform pellet density. This object is generally achieved by preparing pellets at very high pressure and sintering them for a sufficiently long time at an appropriate elevated temperature. It is suggested [27] that a highly pressed pellet acquired a uniform density if its thickness-to-width ratio is less than two (or approximately if t^2/a is less than four in the case

TABLE I

Compound	t^2/a	P ($\times 10^{-9}$ dynes cm^{-2})	d_p (g cm^{-3})	d_x* (g cm^{-3})	Per cent of theoretical density	Pore fraction
$LaCrO_3$	0.100	8.70	4.08	6.773	60.26	0.39
$PrCrO_3$	0.044	9.19	4.28	6.947	61.70	0.38
$NdCrO_3$	0.045	8.20	4.40	7.088	62.14	0.36
$SmCrO_3$	0.035	9.80	4.96	7.352	67.25	0.33
$EuCrO_3$	0.045	9.19	4.78	7.604	62.90	0.37
$GdCrO_3$	0.036	9.19	4.87	7.662	63.62	0.36

*From [4].

TABLE II

Compound	P ($\times 10^{-9}$ dynes cm^{-2})	Per cent of theoretical density acquired	Conductivity at 450 K ($\times 10^{-5}$ Ω cm^{-1})	E_a (eV)
$NdCrO_3$	4.3	61.56	–	–
	6.2	62.00	12.59	0.30
	8.2	62.14	13.48	0.29
	8.6	62.14	–	–
$SmCrO_3$	4.3	66.50	–	–
	6.2	66.56	1.88	0.41
	8.6	67.25	2.11	0.39
	9.7	67.25	2.39	0.38

of circular pellets, where t is the thickness are a is the cross-sectional area). The pellets used in conductivity or Seebeck coefficient measurements were found at pressures above 6×10^8 N m^{-2} and had t^2/a ratios of approximately 0.02 and 0.08, respectively (see Table I). This ensures a uniform pellet density, d_p, which generally lies between 60 and 70% of the theoretical value of crystal density, d_x, of the corresponding material. A fractional change in the density or pore fraction, f, given as

$$f = 1 - d_p/d_x \qquad (3)$$

is generally about 0.35 (see Table I).

The presence of grain boundaries greatly affects the transport behaviour of the material. Russel [28] has shown that in such cases the bulk value of the electrical conductivity, σ, can be given by the relation

$$\sigma = \sigma_p \left(1 + \frac{f}{1 + f^{2/3}}\right) \qquad (4)$$

where σ_p is the experimental value of pellet conductivity and f is given by Equation 3. In order to varify the applicability of Equation 4 the electrical conductivity of few samples of $NdCrO_3$ and $SmCrO_3$, prepared at different pelletizing pressures, has been measured. The log σ against T^{-1} plots obtained from them in the short temperature interval from 400 to 600 K, as shown in Fig. 1, reveal that the dependence of conductivity on pelletizing pressure, P, is more pronounced below 500 K and a pore-faction correction, introduced as in Equation 4, does not appear to be very effective. However, above 500 K, the lines of log σ against T^{-1} plots corresponding to σ-values at different P values are in good agreement. The conductivity values as obtained from these plots at 450 K are given in Table II. The activation energy, E_a, also shows a significant decrease with increasing P for these cases (see Table II). The larger activation energies seen at lower pressures appear, presumably, to be due to larger intercrystalline barriers at the grain boundaries. The dependence of S on P is difficult to determine because of the relatively large (± 5%) error in the experimental values of the former. In this case, no correction for pore fraction has been suggested. The above conclusions on $NdCrO_3$ and $SmCrO_3$ are representative of similar behaviour seen in other $RCrO_3$.

The electric current density, J, was found to be independent of time for all $RCrO_3$. However, its variation with applied electric field, E, is linear, in accordance with Ohm's law, only for low

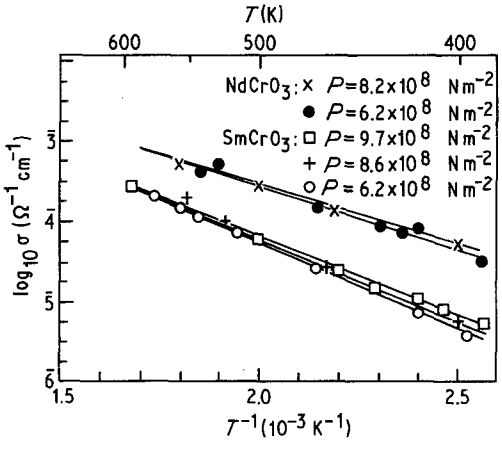

Figure 1 Variation of logarithmic conductivity, σ, with reciprocal of absolute temperature, T, at various pelletizing pressures, P.

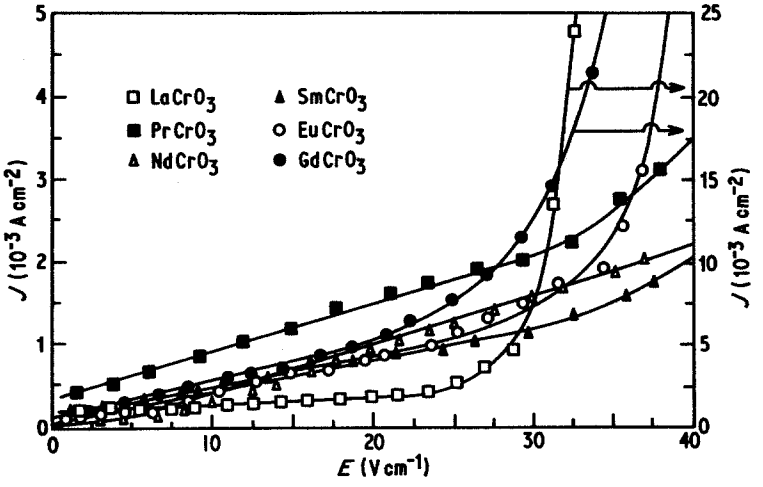

Figure 2 Variation of electric current density, J, with applied electric field, E.

fields, $E \lesssim 25$ V cm^{-1} (see Fig. 2). At higher fields, $E > 25$ V cm^{-1}, the ohmic current is replaced by space-charge limited current and J varies steeply with E. Furthermore, the curves, particularly those of $LaCrO_3$ and $PrCrO_3$, do not necessarily pass through the origin which leaves some doubt as to assigning the contact as true ohmic. E, however, was maintained below 25 V cm^{-1}, where the condition of ohmic contact prevailed.

The a.c. conductivity, σ_{ac}, of some sample pellets of $RCrO_3$ at a constant temperature between 300 and 1000 K was found to be independent of the applied signal frequency (of 10^2 to 10^4 Hz). This was also found to be the case for frequencies of 50 to 10^3 Hz for some heavy $RCrO_3$ [10]. These observations show that grain-boundary effects are insignificant and that σ_{ac} reflects the bulk value of conductivity between 10^2 and 10^4 Hz. The d.c. conductivity, σ_{dc}, at any given temperature was found to be little higher than the value of σ_{ac} at same temperature. This supports the view that the lack of additional resistance in practice is due to the absence of grain boundaries; even if they are present their contribution to the resistance is not very effective, presumably due to the highly conductive nature of $RCrO_3$ and the easy passage of the charge carriers from one grain to another. Besides, the σ-value for a particular $RCrO_3$ at particular temperature, or its variation with temperature, do not differ considerably for samples of different thicknesses. The electrode materials were found to have an insignificant effect on the conductivity. The conductivity was also found to be independent of the shelf-life of the pellet.

The study of the electrical conductivity and the Seebeck coefficient as a function of temperature is the main feature of the present work. The electrical conductivity was found to depend upon the thermal history of the sample. While the nature of the log σT against T^{-1} plots in heating and cooling cycles were found to be very similar in the cases of $RCrO_3$, for R = La, Pr, Nd and Sm, they follow quite different paths in the cases of $EuCrO_3$ and $GdCrO_3$. In the latter cases the transitions observed in the heating cycles have been apparently skipped in the cooling cycles. However, these are repeatable in the successive heating and cooling cycles. The results of electrical conductivity measurements in the first heating cycle at an a.c. signal frequency of 10^3 Hz, have been presented as log σT against T^{-1} plots (Fig. 3) in the studied temperature range. The experimental points are in accordance with Equation 4. The plots reveal that polycrystalline values of conductivity for light $RCrO_3$ are of the order of 10^{-7} Ω^{-1} cm^{-1} and 10^{-1} Ω^{-1} cm^{-1} near room temperature and 1000 K, respectively. Obviously these are semiconducting solids. At 350 K the highest value of about 6.3×10^{-5} Ω^{-1} cm^{-1} has been observed for $LaCrO_3$ and lowest value of about 1.6×10^{-6} Ω^{-1} cm^{-1} has been observed for $SmCrO_3$. An inclusion of the results for $RCrO_3$ (where R = Ho, Yb and Y) studied by Subba Rao *et al.* [10] shows that their conductivities decrease down the series, at least till some temperature well above room temperature. $SmCrO_3$, however, does not conform to this pattern.

The Seebeck coefficients, S, at a particular temperature for each $RCrO_3$ are essentially independent of thermal history and the shelf-life of the pellet, and are reproducible to within

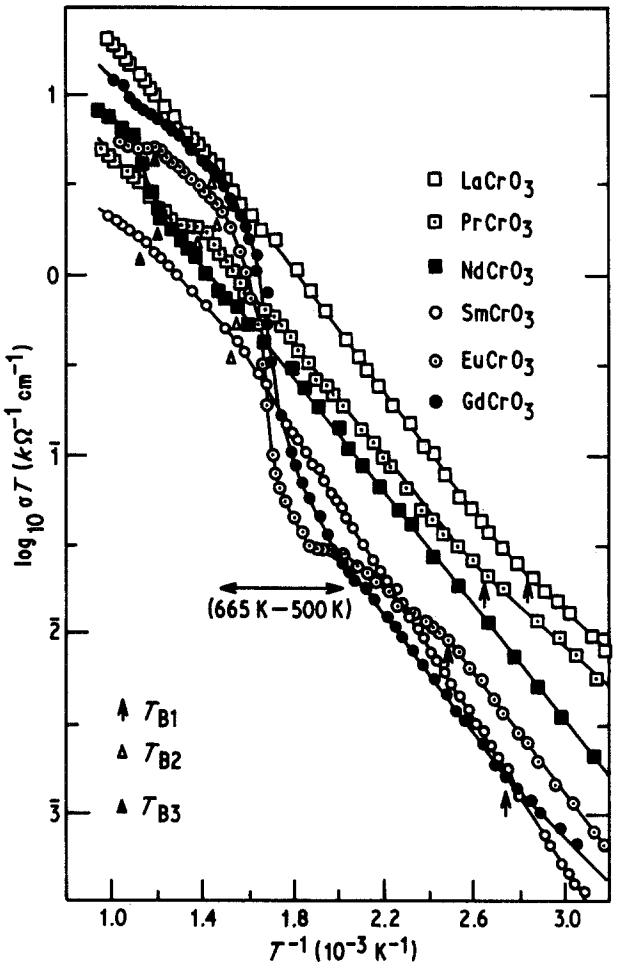

Figure 3 Variation of log σT with inverse of absolute temperature (σ at 1 k Hz).

± 5 %. Nevertheless, a better accuracy in the experiemental points has been observed in the cases of $EuCrO_3$ and $GdCrO_3$. The S against T^{-1} plots (Figs 4 and 5) reveal that the Seebeck coefficient is large, of the order of $1\,mV\,K^{-1}$. Near room temperature the highest value, 0.98 $mV\,K^{-1}$, is obtained for $EuCrO_3$ and the lowest value, $0.75\,mV\,K^{-1}$, is obtained for $NdCrO_3$. Unlike the electrical conductivity, the Seebeck coefficient does not decrease regularly across the $RCrO_3$ series. The sign of S is negative in all cases in the entire temperature range indicating that the change carriers are holes.

It was found that log σT against T^{-1} plots for

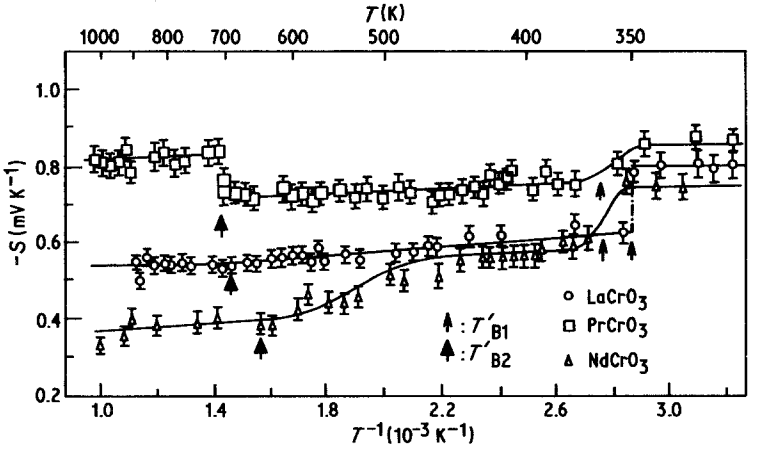

Figure 4 Variation of Seebeck coefficient, S, with inverse of absolute temperature.

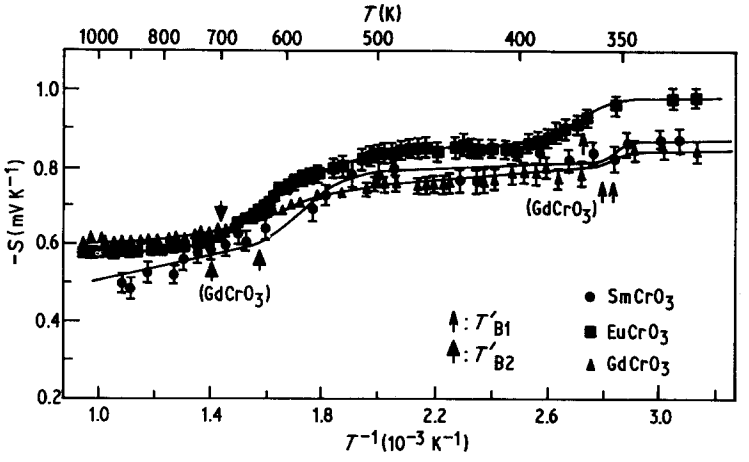

Figure 5 Variation of Seebeck coefficient, S, with inverse of absolute temperature.

$RCrO_3$ are not very similar. The same is also true for S against T^{-1} plots. However, both these plots reveal good correspondance with regard to the changes in nature associated with discontinuity temperatures, T_B and T'_B, respectively. In general, these plots can be divided into three temperature ranges beginning from the low temperature side. These are (1) for $T < T_{B1}$ (or T'_{B1}); (2) for T_{B1} (or T'_{B1}) $\leqslant T \leqslant T_{B2}$ (or T'_{B2}); and (3) for $T < T_{B3}$ (there is no T'_{B3} analogous to T_{B3}). In these temperature ranges the electrical conductivity and the Seebeck coefficient are approximately linear (except in $EuCrO_3$ and $GdCrO_3$ for an interval from 500 to 665 K in the conductivity, and for $NdCrO_3$ to $GdCrO_3$ for an interval from 500 K to T'_{B2} in the Seebeck coefficient measurement) and can be represented by the relations

$$\sigma T = \sigma_{0i} \exp(-E_{ai}/kT) \quad (5)$$

and

$$S = \eta_i T^{-1} + K_i, \quad (6)$$

where $i = 1, 2, 3$ represents the first, second and third temperature ranges, beginning from lower temperature side, T is the absolute temperature, σ_{0i} is the pre-exponential factor, E_{ai} is the activation energy, k is the Boltzmann constant, η_i is the slope and K_i is the intercept of the curve with the S-axis. The summarized results of electrical conductivity and Seebeck coefficient measurements are given in Tables III and IV, respectively.

In order to study the electrical transport influenced by an external magnetic field the magnetoresistances of these compounds have been studied. The magnetoresistance, $\mathscr{M}$, is obtained according to the relation

$$\mathscr{M} = \left(\frac{R_H}{R_0 - 1}\right)_{E_y = 0}, \quad (7)$$

where R_0 and R_H are the resistance of the sample without and with the magnetic field H and E_y is the component of the electric field, E, perpendicular to the direction of the current. With E and H parallel, $\mathscr{M}$ is termed as longitudinal ($\mathscr{M}_\parallel$) and with perpendicular, $\mathscr{M}$ is termed as transverse ($\mathscr{M}_\perp$). Fig. 6 shows that magnetoresistance of $RCrO_3$ above the magnetic ordering temperature (lying well below room temperature for all $RCrO_3$ [29] is not very large. It shows a maximum value for $NdCrO_3$ of about 1.8×10^{-2} at a field 1.0×10^6 A m^{-1}. The lowest value is zero, as observed in the case of $GdCrO_3$. No magnetoresistance has been observed up to 1.28×10^6 A m^{-1} in the cases of $LaCrO_3$ and $PrCrO_3$. $\mathscr{M}_\perp$ and $\mathscr{M}_\parallel$ are both positive for $NdCrO_3$ and $SmCrO_3$ and increase with increasing applied magnetic field.

The dielectric constant, ϵ, of these solids is very high and increases with increasing temperature. The room-temperature value of ϵ for various $RCrO_3$ is given in Table V. The log ϵ against T plots for $RCrO_3$ are very similar; as an illustration, the case of $SmCrO_3$ is shown in Fig. 7 for the temperature range under consideration. In addition to the studies, differential thermal analysis (DTA) of $RCrO_3$ in heating cycles have been carried out in a temperature range from 20 to 700° C, employing a derivatograph from MOM, Budapest, Hungary. In general it is very difficult to determine an exact value of any transition temperature from the DTA traces. Nevertheless, the most probable temperature ranges can be specified and are given

TABLE III Summarized results of electrical conductivity measurements

Compound	$T < T_{B_1}$		T_{B_1} (K)	$T_{B_1} \leqslant T \leqslant T_{B_2}$		T_{B_2} (K)	$T > T_{B_2}$		T_{B_3} (K)
	σ_{0_1} ($K\,\Omega^{-1}\,cm^{-1}$)	E_{a_1} (eV)		σ_{0_2} ($K\,\Omega^{-1}\,cm^{-1}$)	E_{a_2} (eV)		σ_{0_3} ($K\,\Omega^{-1}\,cm^{-1}$)	E_{a_3} (eV)	
$LaCrO_3$	87.17	0.25	350	1107	0.33	685	428	0.28	–
$PrCrO_3$	25.40	0.23	375	214	0.30	720	78.50	0.25	–
$NdCrO_3$	–	–	–	194	0.31	640	127	0.29	850
$SmCrO_3$	–	–	–	212	0.38	650	23.3	0.28	890
$EuCrO_3$	98.50	0.32	400	2.90*	0.20*	500–680†	121‡	0.23‡	836
$GdCrO_3$	4.67	0.25	365	63.13*	0.33*	500–665†	167‡	0.22‡	–

*Calculated for the temperature interval $T_{B_1} < T < 500$ K.
†Temperature interval in which conductivity rises abruptly.
‡Calculated for $T > 680$ K in $EuCrO_3$ and $T > 665$ K in $GdCrO_3$.

TABLE IV Summarized results of Seebeck coefficient measurements

Compound	$T < T'_{B_1}$		T'_{B_1} (K)	$T'_{B_1} \leqslant T \leqslant T'_{B_2}$		T'_{B_2} (K)	$T > T'_{B_2}$	
	η_1 (V)	K_1 ($mV\,K^{-1}$)		η_2 (V)	K_2 ($mV\,K^{-1}$)		η_3 (V)	K_3 ($mV\,K^{-1}$)
$LaCrO_3$	0	0.81	350	0.06	0.43	685	0.02	0.54
$PrCrO_3$	0	0.87	365	0.04	0.65	715	0.03	0.79
$NdCrO_3$	0	0.75	355	0.03*	0.49*	635†	0.06	0.31
$SmCrO_3$	0	0.86	350	0.05*	0.69*	630†	0.18	0.32
$EuCrO_3$	0	0.98	370	0.06*	0.71*	715†	0.06	0.52
$GdCrO_3$	0	0.86	360	0.07*	0.61*	690†	0.05	0.55

*Calculated for the temperature $T'_{B_1} < T < 500$ K.
†The magnitude of S begins to fall from 500 K for $NdCrO_3$ and $SmCrO_3$ and from ~ 550 K for $EuCrO_3$ and $GdCrO_3$. This fall continues until T'_{B_2} is reached.

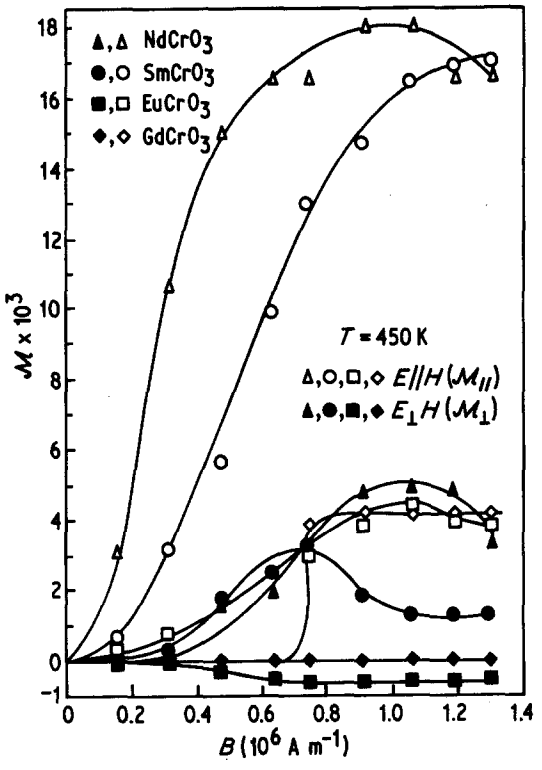

Figure 6 Variation of magnetoresistance, $\mathcal{M}$, with applied magnetic field, B ($T = 450$ K).

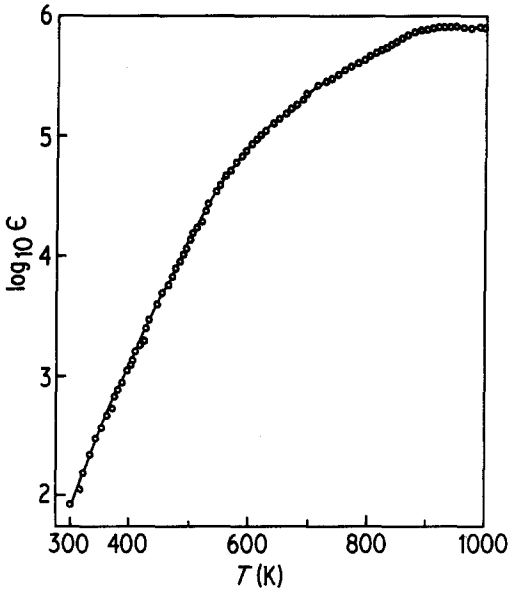

Figure 7 Log ϵ against temperature plot for $SmCrO_3$.

in Table VI. Generally, these ranges lie between 220 and 300° C.

4. Discussion

Among the $RCrO_3$ studied, the electrical conductivity measurements have been carried out on various forms of pure $LaCrO_3$: as the fused sample [6], sintered polycrystalline sample [6–13], single crystal [10] and also a doped material [9, 11, 12]. The maximum conductivity and minimum activation energy is obtained for the crystal of $LaCrO_3$ as pure material. However, the conductivity can be controlled by the doping of impurities in the appropriate composition form. Considerable difference has been observed in the activiation energy, E_a, which is found, generally to be of the order of 0.2 eV. In addition, there is much uncertainty in the conductivity discontinuities. The summarized results of previous work are presented in Table VII. In general, our results for $LaCrO_3$ agree fairly well with those earlier reported: however, differences occur regarding the conductivity discontinuities and activation energies. We observed the first discontinuity at 350 K and the second at 685 K. The activation energies in the different temperature regions beginning from the lower temperature side are 0.25 eV, 0.33 eV and 0.28 eV (see Table III). The ohmic contact in $RCrO_3$ was found to hold true in general at lower fields; $E \lesssim 25\ V\ cm^{-1}$. Therefore, any measurement made beyond this field is bound to give a different result. A difference in the values of E_a observed by various workers appears to be due presumably to this contact problem. Among other light $RCrO_3$ in pure form the conductivity of $PrCrO_3$ has been measured by Subba Rao *et al.* [10]. They found the conductivity to be higher than that of polycrystalline $LaCrO_3$ at temperatures below 500 K. However, a lowering appears at higher temperatures. They report a conductivity discontinuity near 803 K. In our measurements the conductivity of $PrCrO_3$ is always smaller than that of $LaCrO_3$ and the log σT against T^{-1} plot (Fig. 3) shows two discontinuities, one at 375 K and the other at 720 K.

For all the studied $RCrO_3$ the current density, J, is essentially independent of time and σ_{dc} is

TABLE V

Compound	$LaCrO_3$	$PrCrO_3$	$NdCrO_3$	$SmCrO_3$	$EuCrO_3$	$GdCrO_3$
ϵ	57	32	20	64	32	23

TABLE VI

Compound	Anomalous range in DTA trace (° C)	Probable transformation temperature (K)
$LaCrO_3$	240–300	533
$PdCrO_3$	220–280	513
$NdCrO_3$	220–280	–
$SmCrO_3$	–	573
$EuCrO_3$	220–300	543
$GdCrO_3$	–	533

greater than σ_{ac} at any temperature. This is indicative of the absence of ionic conduction in them, at least in the temperature range 300 to 1000 K. A similar conclusion was drawn by Webb *et al.* [11] but an estimation of ionic conduction on the basis of a.c. and d.c. values of σ, as made by Subba Rao *et al.* [10] does not appear convincing.

In order to describe the conduction mechanism in the studied materials a suitable model must be used. Let us first try to discuss it on the basis of an energy band model. The relevant energy states or bands for conduction in $RCrO_3$ are: filled oxygen O^{2-}:2p band, R^{3+}:4f levels (or extremely narrow bands), partially-filled Cr^{3+}:3d narrow bands, R^{2+}:$4f^{n+1}$ levels (or extremely narrow bands) and the empty Cr^{3+}:4s band. The magnitude of the electrical conductivity in the studied $RCrO_3$ is found to be slightly greater than that in Cr_2O_3 and is many orders of magnitude larger than in the corresponding R_2O_3 [30, 31]. Elimination of the R^{3+} band leaves O^{2-}:2p; Cr^{3+}:3d and Cr^{3+}:4s bands as the relevant bands for conduction. The crystal field also splits the 3d band into e_g and t_{2g} sub-bands [32]. In order to recognize the effective bands and to know their relative position one can use the semi-empirical model proposed by Goodenough [32] and a scale plot of energy bands proposed by Howng and Thorn [33]. However, both are specificially drawn for $LaCrO_3$. As all $RCrO_3$ are similar in structure and energy bands associated with rare-earth ions are not relevant for electrical conduction in them, the above models should be valid for each $RCrO_3$ with little modification in the relative position of their bands. Considering the above facts, the general schematic band diagram for $RCrO_3$ can be drawn, as depicted in Fig. 8. According to this band diagram, the O^{2-}:2p band is lowest and is about 5 eV below the Cr^{3+}:4s band. The e_g sub-band lies below the Cr^{3+}:4s band and is separated from the t_{2g} sub-band by nearly 2 eV in the case of $LaCrO_3$. The t_{2g} sub-band can, at most, accommodate six electrons. However, in the Cr^{3+} ion only three 3d electrons are available. Therefore, the t_{2g} sub-band will be partially filled. According to the simple band theory, this band being the partially-filled uppermost band should support a metallic conduction. However, no such behaviour has been revealed by $RCrO_3$. This indicates that the t_{2g} sub-band is extremely narrow and correlation effects make all the electrons localized. Obviously, this band cannot support any band conduction. The Fermi energy level, therefore, lies between the empty Cr^{3+}:3d (e_g) and Cr^{3+}:3d (t_{2g}) sub-bands.

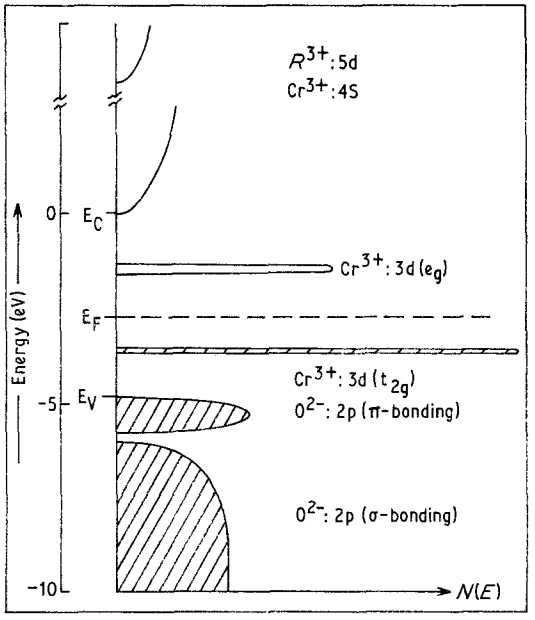

Figure 8 Schematic band diagram for $RCrO_3$.

Based upon the energy band diagram, the intrinsic conduction can be suggested to occur via the following processes:

(a) Electrons excited from the O^{2-}:2p band to the conduction Cr^{3+}:4s band creating holes in the former.

(b) Electrons excited from the O^{2-}:2p band to the Cr^{3+}:3d (e_g) sub-band leaving holes in the former.

(c) Electrons excited from the Cr^{3+}:t_{2g} states to the narrow Cr^{3+}:3d (e_g) sub-band, leaving holes in the former.

(d) Electrons exctied from the Cr^{3+}:t_{2g} sub-band to the Cr^{3+}:4s band, leaving holes in the former.

The above conduction processes can be analyzed on the basis of activation energy considerations

TABLE VII *Comparison of previous data for electrical conductivity of* $LaCrO_3$

Sample number	Sample	Conductivity discontinuity temperature, T(K)		Activation energy, E_a (eV)	Mobility, μ ($cm^2\ V^{-1}\ sec^{-1}$)	Density of the charge carriers, n (cm^{-3})	Reference
		I	II				
1	Fused sample	560	1000	0.60	0.6 ($T = 350$ K)	2.0×10^{15}	[6]
2	Ceramic	560	1000	–	–	–	[6]
3	Ceramic	–	–	0.55	–	–	[9]
4	Ceramic	450	–	0.18	5.2×10^{-4} ($T = 295$ K)	5.0×10^{19}	[11]
5	Ceramic	–	–	0.19	–	–	[12]
6	Single crystal	–	–	0.08	–	–	[10]
7	Ceramic	–	–	0.22	–	–	[10]
8	Ceramic	350	685	0.25 ($T < 350$ K) 0.33 (350–685 K) 0.28 ($T > 685$ K)	2.2×10^{-2} ($T = 325$ K)	3.1×10^{18}	Present study

and the nature of the majority conduction charges these envoke. The experimentally observed activation energy in $R\mathrm{CrO_3}$ is nearly 0.3 eV, but Processes a and b suggest a much larger (above 1 eV) value. Subba Rao *et al.* [10] find on the consideration of electronic spectra of $R\mathrm{CrO_3}$ and the model of Goodenough that the minimum energy required would be 1 eV if any intrinsic conduction were existed. Processes c and d suggest electrons as the dominating charge carriers, but the Seebeck coefficient suggests holes as the dominating charge carriers, in the entire temperature range under consideration. Thus, ruling out Processes a and b directly on the basis of activation energy considerations and Processes c and d on the basis of their activation energy as well as on the nature of their dominating charge consideration one can directly rule out a band type intrinsic conduction in $R\mathrm{CrO_3}$. Furthermore, in support, the pre-exponential constants, σ_{0i}, calculated from $\log \sigma T$ against T^{-1} plots were also found to be very small (Table III). These are much smaller than the value one expects for the band-type conduction.

A probable hopping mechanism, given as $\mathrm{Cr^{3+} + Cr^{3+} \rightarrow Cr^{4+} + Cr^{2+}}$ has also been ruled out [33] due to energy and nature of the charge carrier considerations. It is an electron-dominating process and requires an energy that is half the difference between fourth and third ionization energies of the chromium ion. This energy is nearly 9 eV [34]. Obviously, it is very large in comparison to the observed activation energies, so this process is not feasible. Ruling out the intrinsic band or hopping conduction on the basis of above arguments, one is forced to think that the conduction is extrinsic, which may be either band-type or hopping-type. The slopes of S against T^{-1} plots (see Table IV) are found to be very small and correspond to an energy of 0.05 eV. However, E_a estimated from conductivity data is nearly 0.3 eV (Table III). The large difference between these energies suggests that the mobility of the charge carriers is thermally activated. Furthermore, up to about 350 K a constant Seebeck coefficient of the studied $R\mathrm{CrO_3}$ suggests a constancy in the number of charge carriers. At higher temperatures thermal generation of the charge carriers takes place, but their number is very small in comparison to the number of the charge carriers already present at any lower temperature. These facts suggest that even the extrinsic conduction is not band-type. Therefore, the impurity centres responsible for the electrical conduction cannot be pictured as the donor or accepter centres.

Subba Rao *et al.* [10] have suggested the existence of a large number of $\mathrm{Cr^{4+}}$ centres due to the native defects in $R\mathrm{CrO_3}$ and the conduction of holes from these centres to neighbouring $\mathrm{Cr^{3+}}$ sites. It is well known that $\mathrm{Cr_2O_3}$ and other transition metal oxides tend to be cation deficient [35]. $R\mathrm{CrO_3}$ seem to retain this tendency. If this is so, each trivalent cation deficiency needs three holes to compensate for the charge neutrality of the material and, hence, it would be capable of producing three $\mathrm{Cr^{4+}}$ centres according to the process,

$$X^{3+} \rightarrow X^0 + 3[h]$$

$$3\mathrm{Cr^{3+}} + 3[h] \rightarrow 3\mathrm{Cr^{4+}}, \qquad (8)$$

where X^{3+} is a trivalent cation and $[h]$ is the hole it leaves back. Indeed, the presence of a $\mathrm{Cr^{4+}}$ centre seems a reasonable proposal to accept.

The electrical conductivity resulting from the $\mathrm{Cr^{4+}}$ centres may be given by the expression

$$\sigma = \frac{n e^2 a_0^2 \nu_0}{kT} \exp\{-E_a/kT\}, \qquad (9)$$

where n is the number of $\mathrm{Cr^{4+}}$ centres per unit volume at a certain temperature T, a_0 is the minimum distance between the neighbouring $\mathrm{Cr^{3+}}$ centres and ν_0 is the hopping frequency that corresponds to the optical phonon frequency. From the known structure of $R\mathrm{CrO_3}$ at room temperature one can evaluate a_0. Knowing the order of ν_0 (of about 10^{13} Hz) from the literature [12, 35], and σ and E_a from our experimental data, the approximate value of n can be obtained. It is observed that n is of the order of 10^{18} per $\mathrm{cm^3}$ (see Table VIII), which is a reasonable value.

For a hopping mechanism, the Seebeck coefficient, S, is independent of temperature and its magnitude primarily depends upon the density of the charge carriers. It is expressed in the form of the Heikes formula [37],

$$S = \frac{k}{e}\left(\frac{S_R^*}{k} - \log_e \frac{c}{1-c}\right), \qquad (10)$$

where S_R^* is the effective entropy of the lattice which is temperature independent and S_R^*/k is very small. c is given by n/N_s, where n is the number of carriers in the states and N_s is the total number of available states. Neglecting the term

TABLE VIII Calculated values of n and calculated and experimentally determined values of S at 325 K

Compound	n^* ($\times 10^{-18}$ cm^{-3})	$N_s^\dagger$ ($\times 10^{-22}$ cm^{-3})	$-S$ (mV K^{-1})	
			Calculated	Experimental
$LaCrO_3$	3.10	1.707	0.74	0.81
$PrCrO_3$	0.99	1.737	0.84	0.87
$NdCrO_3$	5.97	1.748	0.69	0.75
$SmCrO_3$	6.14	1.769	0.68	0.86
$EuCrO_3$	3.69	1.818	0.73	0.98
$GdCrO_3$	1.78	1.794	0.79	0.86

*Calculated from conductivity data.
†Calculation from composition and X-ray density.

S_R^*/k from the relation gives

$$S = \frac{k}{e} \log_e \left(\frac{1}{c} - 1 \right) \tag{11}$$

or

$$S = \frac{k}{e} \log_e \left(\frac{N_s}{n} - 1 \right). \tag{12}$$

The values of N_s can be obtained from the composition and X-ray density of a particular $RCrO_3$. N_s is of the order of 10^{22} cm^{-3} (see Table VIII). The calculated and experimental values of S for different $RCrO_3$ at 325 K are also given in Table VIII and there is a good agreement between them. This further strengthens the idea of electrical conduction by the hopping of the holes localized at the Cr^{4+} sites.

The mobility of the charge carriers, μ, can be evaluated from the relation

$$\mu = \frac{e a_0^2 \nu_0}{kT} \exp(-E_a^\mu / kT), \tag{13}$$

where E_a^μ is the mobility activation energy expressed by the relation

$$E_a^\mu = E_a - e\eta, \tag{14}$$

where η is the slope of the S against T^{-1} plot. In Table IX the values of E_a^μ and μ are given at various temperatures. It is observed that at 325 K, μ lies in the range 2.0×10^{-4} to 4.4×10^{-2} (cm^2 V^{-1} sec^{-1}) for the studied $RCrO_3$. This is just of the order one expects for the hopping condition.

The discontinuity temperatures T'_{B1} (or T'_{B2}) at which the major Seebeck coefficient change occurs are, however, different in different $RCrO_3$, yet these fall in a short interval of temperature (Table IV). A similar trend is observed in the case of conductivity breaks. In a few cases it has been possible to determine the exact value of the discontinuity temperatues, but in others only a range in which some anomalies in S or σ occur can be shown. In most cases there exists only a small difference in the values of T_{B1} and T'_{B1} or T_{B2} and T'_{B2}. It is due to the basic difference in the thermal conditions of the sample and the measuring technique. In the conductivity measurement the sample acquires a uniform temperature throughout while in the Seebeck coefficient measurement the sample is under a temperature difference of nearly 15° C and, hence, the temperature at which the conduction undergoes some change would be first acquired by the hot end, but the discontinuity temperature is the average of the temperature of the hot and cold end which would be little below the actual discontinuity temperature. Hence, a small difference in T_B and T'_B can be practically ignored. We believe that the corresponding conductivity and Seebeck coefficient discontinuity temperatures reflect similar anomalies in these solids. We shall attempt to classify qualitatively whether the anomaly is due to a change in crystal structure, a phase transition, a change in the conduction mechanism, a dielectric anomaly or a change in the magnetic ordering etc.

For all the studied $RCrO_3$ the Seebeck coefficient is constant below T'_{B1}, but shows sudden drop at this temperature (Figs 4 and 5). The conductivity plots (Fig. 3) for La, Pr, Eu and Gd orthochromites also, reveal a break at T_{B1}. In all cases T_{B1} and T'_{B1} are nearly equal except for $EuCrO_3$ where these differ by about 30 K. No conductivity break close to T'_{B1} appears in the cases of $NdCrO_3$ and $SmCrO_3$. The magnetic ordering temperature for all $RCrO_3$ is well below room temperature [29]. Therefore, these breaks cannot be assigned to a magnetic ordering in these solids. Besides, no phase transition occurs near these breaks; the DTA of $RCrO_3$ also supports this fact. Hence, the only reasonable possibility is

TABLE IX Values of the mobility activation energy, E_a^{μ} (eV) and mobility, μ ($cm^2\ V^{-1}\ sec^{-1}$) at various temperatures

Compound	325 K		450 K		650 K		750 K		850 K		950 K	
	E_a^{μ} (eV)	μ ($cm^2\ V^{-1}\ sec^{-1}$)	E_a^{μ} (eV)	μ ($cm^2\ V^{-1}\ sec^{-1}$)	E_a^{μ} (eV)	μ ($cm^2\ V^{-1}\ sec^{-1}$)	E_a^{μ} (eV)	μ ($cm^2\ V^{-1}\ sec^{-1}$)	E_a^{μ} (eV)	μ ($cm^2\ V^{-1}\ sec^{-1}$)	E_a^{μ} (eV)	μ ($cm^2\ V^{-1}\ sec^{-1}$)
$LaCrO_3$	0.25	0.022	0.27	0.110	0.27	0.65	0.26	1.25	0.26	1.78	0.26	2.31
$PrCrO_3$	0.23	0.044	0.26	0.141	0.26	0.77	0.22	2.30	0.22	3.03	0.22	3.72
$NdCrO_3$	0.31	0.002	0.28	0.084	0.23	1.31	0.23	1.96	–	–	0.55	2.95
$SmCrO_3$	0.38	0.002	0.33	0.023	0.10	1.32	0.10	1.46	0.10	1.54	–	–
$EuCrO_3$	0.32	0.002	0.14	0.032	–	–	0.17	7.69	–	–	–	–
$GdCrO_3$	0.25	0.021	0.27	0.107	–	–	0.17	4.90	0.17	5.89	0.17	6.73

that of a dielectric anomaly or an electrical change of different kind.

The next break temperatures T_{B2} and T'_{B2} or the range of temperature in which the anomalies in σ and S plots do occur are given in Tables III and IV, respectively. It is observed from S against T^{-1} plots that while for $LaCrO_3$ a variation occurs only in its slope, there also exists a sharp change in the magnitude of S in the case of $PrCrO_3$ and a gradual drop above 500 K in $NdCrO_3$ and $SmCrO_3$ and above 545 and 550 K in the cases of $EuCrO_3$ and $GdCrO_3$, respectively. This drop continues till T'_{B2}. Among the studied $RCrO_3$ it appears that $EuCrO_3$ and $GdCrO_3$ are particularly sensitive to the cause raising the electrical anomalies. An abrupt rise in the electrical conductivity has been observed in their cases in the temperature range 500 to 680 K. The DTA (Table VI) of $RCrO_3$ suggests some phase transformation between 520 and 580 K. The transformation temperatures at which the crystal structure may change from orthorhombic to rhombohedral appear near 545 to 535 K, respectively. These values fall well within the temperature range (500 to 680 K) in which the conductivity anomalies appear. Hence, the anomalies in these cases can be related to a change in the structure. In the cases of remaining $RCrO_3$, T_{B2} or T'_{B2} is well above transformation temperature. Therefore these discontinuities are not due to a structural transformation, but presumably due to some kind of change in the electrical conduction mechanism. Here it would be interesting to note that there is some difference in the nature of the anomalies in σ and S in the cases of $NdCrO_3$ and $SmCrO_3$. While a distinct break appears in the conductivity plot at 640 K for $NdCrO_3$ and at 625 K for $SmCrO_3$, S has a slow drop from 500 to 635 K and 500 to 630 K in the respective cases. DTA anomalies in their cases lie in these temperature ranges and there is a fair probability that the anomalies in the nature of the S against T^{-1} plots in these cases are also due to structural transformations. Their conductivities, however, do not seem to be affected by these changes. Subba Rao *et al.* [10] have related the conductivity breaks of some heavy $RCrO_3$ to a ferroelectric–paraelectric transformation. Our attempt to perform dielectric measurements at higher temperatures to see whether some dielectric anomaly occurs near the discontinuity temperature failed because $RCrO_3$ are very lossy. The distorted chromium oxygen polyhedra, believed to be the origin of ferroelectricity in $RCrO_3$, reveal increasing distortion from La to Lu. One can also think that these reasons may account for the anomalies in the conductivities of $EuCrO_3$ and $GdCrO_3$.

From our electrical conductivity and Seebeck coefficient data a fact common to all $RCrO_3$ is that, above a specific temperature (lying between 625 and 700 K) there appears a linear variation in the plots of log σT against T^{-1} and S against T^{-1}. Obviously, these temperatures are too high to be related to the phase transitions. The difference in the slopes of log σT against T^{-1} and S against T^{-1} plots (correspondingly in the activation energies) still indicates that the charge carriers continue to have a thermally-activated mobility. However, there is a drop in the mobility activation energy, E^{μ}_{a}, for all $RCrO_3$ at higher tempertures (Table IX). This lowering in E^{μ}_{a} is probably brought about by the reduction in the potential barriers between Cr^{4+} and Cr^{3+} sites due to the presence of some holes in the thermally-excited states at the Cr^{4+} sites. However, a large reduction in E^{μ}_{a} is expected if the bulk holes, being freed from their sites with the rise in temperature, take over the conduction above T_{B2}. The difference in the values of E^{μ}_{a} for $LaCrO_3$ and $PrCrO_3$ just above and below T_{B2} is not very large. It appears, therefore, at least in these cases, that the holes freed above T_{B2} are very small in number and that the major contribution continues to come from the hopping of the holes from Cr^{4+} to Cr^{3+} sites. It has been observed that in the remaining $RCrO_3$ there is very large reduction in the values of E^{μ}_{a} at higher temperatures. E^{μ}_{a} almost vanishes in the cases of $SmCrO_3$ and $EuCrO_3$ as the temperature approaches 1000 K. This is probably due to the smoothing of the potential barriers by thermal fluctuations leading to the freeing of holes in increasing numbers at higher temperatures.

Acknowledgements

This work has been supported by CSIR, India. One of us (AKT) is thankful to the Council for financial assistance. The authors are also grateful to Dr D.C. Agrawal of Department of Materials Sciences, I.I.T., Kanpur for providing DTA facilities.

References

1. S. GELLER and E. A. WOOD, *Acta Cryst.* 9 (1956) 563.

2. S. GELLER, *ibid.* **9** (1956) 1019.
3. *Idem, J. Chem. Phys.* **24** (1956) 1236.
4. *Idem, Acta Cryst.* **10** (1957) 243.
5. G. V. SUBBA RAO, G. V. CHANDRASEKHAR and C. N. R. RAO, *Sol. State. Commun.* **6** (1968) 177.
6. J. S. RUIZ, A. M. ANTHONY and M. FOEX, *Compt. Rend.* **264B** (1967) 1271.
7. M. FAUCHER, F. CABANNES and A. M. ANTHONY, *ibid*. **264B** (1967) 1671.
8. J. ELSTON, Z. MIHAILOVIC and M. ROUX, *Proc. Symp. Salzburg Austria* **3** (1966) 389.
9. D. B. MEADOWCROFT, *J. Phys. D.* **2** (1969) 1225.
10. G. V. SUBBA RAO, B. M. WANKLYN and C. N. R. RAO, *J. Phys. Chem. Sol.* **32** (1971) 345.
11. J. B. WEBB, M. SAYER and A. MANSINGH, *Canadian J. Phys.* **55** (1977) 1725.
12. D. P. KARIM and A. T. ALDRED, *Phys. Rev. B* **20** (1979) 2225.
13. A. K. TRIPATHI and H. B. LAL, *Mater. Res. Bull* **15** (1980) 233.
14. M. FOEX, *C. R. Acad Sci (France)* **26** (1965) 6989.
15. H. B. LAL, V. PRATAP and A. KUMAR, *Pramana (India)* **9** (1978) 409.
16. B. K. VERMA, V. PRATAP and H. B. LAL, *Indian J. Pure and Appl. Phys.* **18** (1980) 150.
17. H. B. LAL and R. N. PANDEY, *Z. Naturforsch* **33a** (1978) 1035.
18. A. K. TRIPATHI and H. B. LAL, *J. Phys. Soc. Japan* **49** (1980) 1896.
19. H. B. LAL and V. PRATAP, *J. Mater. Sci.* **17** (1982) 377.
20. B. K. VERMA and H. B. LAL, *J. Phys. C.* **11** (1978) 5035.
21. N. DAR and H. B. LAL, *Mater. Res. Bull.* **14** (1979) 1263.
22. H. B. LAL, *J. Mag. and Mag. Mater.* **23** (1981) 41.
23. H. B. LAL and M. SINGH, *J. Phys. C.* **14** (1981).
24. V. R. VADAV and H. B. LAL, *Canadian J. Phys.* **57** (1979) 1204.
25. *Idem, Japan, J. Appl. Phys.* **12** (1979) 2229.
26. K. SHAHI, H. B. LAL and S. CHANDRA, *Indian J. Pure and Appl. Phys.* **13** (1975) 1.
27. R. KUMAR, *Sci. Reporter* 8 (1971) 568.
28. H. W. RUSSEL, *J. Amer. Ceram. Soc.* **18** (1935) 1.
29. R. ALEONARD, R. PAUTHENET, J. P. REBOUILLAT and V. ZARIBOCKJA, *CR Acad Sci (Paris)* **262B** (1966) 799.
30. G. V. SUBBA RAO, S. RAMDAS, P. N. MEHROTRA and C. N. R. RAO, *J. Sol. Stat. Chem.* **2** (1970) 377.
31. A. KUMAR, PhD thesis, University of Gorakhpur, India (1975).
32. J. B. GOODENOUGH, *J. Appl. Phys.* **37** (1966) 1415.
33. W. Y. HOWNG and R. J. THORN, *J. Phys. Chem. Sol.* **41** (1980) 75.
34. D. ADLER, in "Physics of Electronic Ceramics Part A" edited by L. L. Hench and L. B. Dov. (1971) p. 29.
35. J. B. GOODENOUGH, in "Progress in Solid State Chemistry" Vol. 5, edited by H. Reiss (Pergamon Press, Oxford and New York, 1972) p. 145.
36. P. DOIUGIER and P. HAGENMULLER, *J. Sol. Stat. Chem.* **11** (1974) 177.
37. R. R. HEIKES, in "Thermoelectricity" edited by R. R. Heikes and R. W. Ure (Wiley Interscience New York, 1961) p. 45.

Received 2 October
and accepted 4 November 1981